Speract induces calcium oscillations in the sperm tail

Chris D. Wood, Alberto Darszon, and Michael Whitaker

School of Cell and Molecular Biosciences, University of Newcastle upon Tyne, NE2 4HH, UK

Sea urchin sperm motility is modulated by sperm-activating peptides. One such peptide, speract, induces changes in intracellular free calcium concentration ($[Ca^{2+}]_i$). High resolution imaging of single sperm reveals that speract-induced changes in $[Ca^{2+}]_i$ have a complex spatiotemporal structure. $[Ca^{2+}]_i$ increases arise in the tail as periodic oscillations; $[Ca^{2+}]_i$ increases in the sperm head lag those in the tail and appear to result from the summation of the tail signal transduction events. The period depends on speract concentration. Infrequent spontaneous $[Ca^{2+}]_i$ transients were also seen in the tail of unstimulated sperm, again with the head lagging the tail. Speract-induced fluc-

tuations were sensitive to membrane potential and calcium channel blockers, and were potentiated by niflumic acid, an anion channel blocker. 3-isobutyl-1-methylxanthine, which potentiates the cGMP/cAMP-signaling pathways, abolished the $[Ca^{2+}]_i$ fluctuations in the tail, leading to a very delayed and sustained $[Ca^{2+}]_i$ increase in the head. These data point to a model in which a messenger generated periodically in the tail diffuses to the head. Sperm are highly polarized cells. Our results indicate that a clear understanding of the link between $[Ca^{2+}]_i$ and sperm motility will only be gained by analysis of $[Ca^{2+}]_i$ signals at the level of the single sperm.

Introduction

Two sea urchin jelly coat sperm-activating oligopeptides, speract (*Strongylocentrotus purpuratus*) and resact (*Arbacia punctulata*), are thought to be responsible for sperm-egg chemotaxis, based on the observation that sperm will swarm to a resact-filled pipette (Ward et al., 1985; Cook et al., 1994). Chemotactic responses are postulated to comprise alterations in the sperm's flagellar beat asymmetry and curvature; these alterations can be induced in demembranated sperm by calcium addition (Brokaw, 1979, 1987). Moreover, resact-induced chemotaxis is dependent on external calcium (Ward et al., 1985). Hyperactivation of mammalian sperm is accompanied by oscillations in intracellular free calcium concentration ($[Ca^{2+}]_i$)* that track the flagellar beat (Suarez et al., 1993). It has been shown that speract induces $[Ca^{2+}]_i$ increases in suspensions of sea urchin sperm labeled with calcium indicator dyes (Schackmann and Chock, 1986; Babcock et al., 1992). There is evidence that the $[Ca^{2+}]_i$ increase alters the pattern of motility in *A. punctulata* sperm, consistent with a role in chemotaxis (Kaupp et al., 2003). However, sea urchin sperm are highly differentiated cells with a marked cell polarity. The speract receptor is localized to the sperm tail (Cardullo et al., 1994), which also contains the axoneme, the organelle of motility. It is highly likely that signaling in the sperm tail is central to motility regulation. Significantly, the tail represents a very small proportion of the total sperm volume.

We undertook high resolution imaging of single sperm to determine whether the measurements of $[Ca^{2+}]_i$ in sperm suspensions reflected changes in the sperm head, the sperm tail, or a combination of the two. We found that the earlier measurements by ourselves and others largely reflected $[Ca^{2+}]_i$ changes in the head (Schackmann and Chock, 1986; Babcock et al., 1992; Kaupp et al., 2003). Our spatially resolved measurements also revealed previously undiscovered calcium fluctuations in the sperm tail, both spontaneous and speract-dependent. Experiments with ion channel blockers demonstrate that the speract-induced fluctuations are regulated by mechanisms originally uncovered from experiments on sperm suspensions. Thus, speract-induced $[Ca^{2+}]_i$ fluctuations are the single cell response that underlies the characteristics of the bulk $[Ca^{2+}]_i$ responses measured in sperm suspensions. The spontaneous $[Ca^{2+}]_i$ fluctuations, interestingly, do not share this pharmacology and are thus a second new and independent phenomenon. Given these observations, further insights into regulation of $[Ca^{2+}]_i$-modulated sperm
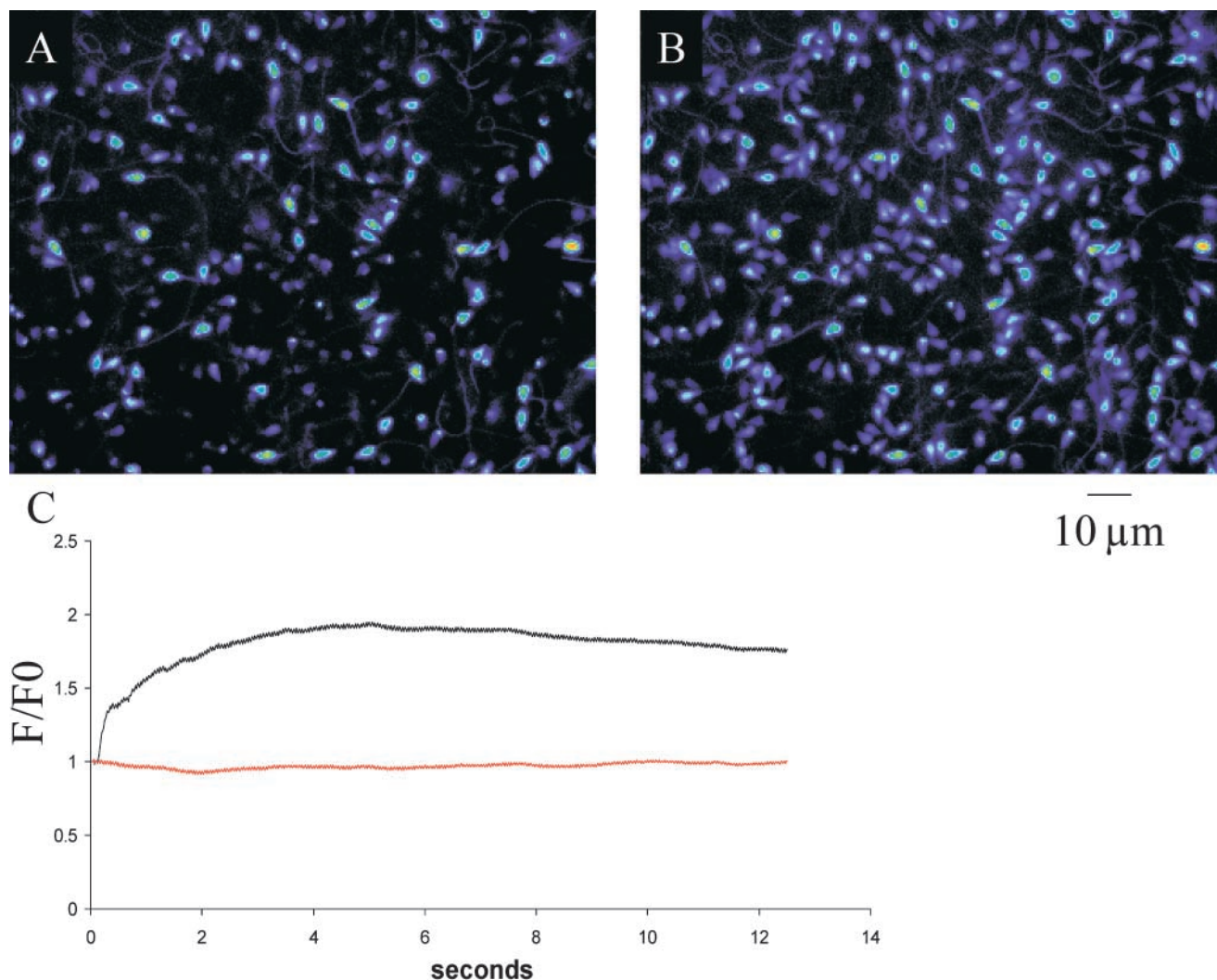
Figure 1. **Typical response of a field of sperm to addition of speract to a final concentration of 125 nM.** (A) Fluo-4 fluorescence immediately before speract addition. (B) Fluo-4 fluorescence 4 s after speract addition. Images extracted from a time series acquired at 40 frames per second with 25-ms individual frame exposure time. (C) Ratio increases in Fluo-4 fluorescence across whole field. Upper trace (black), response to addition of 125 nM speract at t = 0. Lower trace (red), fluorescence from control field with no speract addition. Both traces have been corrected for the effects of fluorophore bleaching. Data acquired at 40 frames per second with 25-ms individual frame exposure time.

motility are likely to be achieved primarily at the level of single sperm.

Results

Saturating concentrations of speract ($\sim$100 nM) induce an approximately fivefold transient increase in $[Ca^{2+}]_i$ in Fura-2– or Fluo-3–loaded *S. purpuratus* sea urchin sperm bulk suspensions (Cook and Babcock, 1993a,b). From these previous studies, it was determined that $[Ca^{2+}]_i$ elevates with a time to half-height ($t_{1/2}$) of $\sim$0.4 s and relaxes almost to the basal level with a $t_{1/2}$ of $\sim$25 s (Schackmann and Chock, 1986; Babcock et al., 1992; Nishigaki et al., 2001). To study the spatial distribution of this transient within single sperm, a system has been developed for measuring, continuously and at relatively high sampling frequencies (40 frames.s^{-1}), spatially resolved $[Ca^{2+}]_i$ changes (see Materials and methods and Fig. 1). This approach yields data consistent with the changes in calcium that have been measured in sperm popu-

lations, yet has uncovered a temporal and spatial structure to sperm calcium signals that was not predicted and is only apparent at the single-cell level.

Speract addition increases intracellular calcium in immobile sperm

Fluo-4 was chosen as a Ca^{2+} indicator dye for the present work because of its high quantum yield. When labeled sea urchin sperm are attached to a poly-L-lysine–treated coverslip and imaged under an inverted microscope coupled to a fast and highly sensitive CCD camera, two main sperm populations can be distinguished: cells that are only slightly fluorescent (15–85% of total, median 44%, $n = 18$), and very bright cells (Fig. 1 A). The former represent cells with low resting calcium levels and the latter, cells with high resting levels. There was no significant correlation between resting calcium level and whether the cells had undergone the acrosome reaction; assessed from 10 separate batches of sperm, 19.3 $\pm$ 3.5% of cells with low resting $[Ca^{2+}]_i$ versus

$28.9 \pm 5.3\%$ of cells with high resting $[Ca^{2+}]_i$ had undergone the acrosome reaction ($\pm$ SEM, P > 0.05; unpaired two-tailed t test). Many of the cells with high resting $[Ca^{2+}]_i$ (>60%) are swollen, and it is likely that they are unable to properly regulate $[Ca^{2+}]_i$. The fluorescence from these bright cells never varies significantly over the course of the experiment, and this population does not respond to speract.

Sperm with low resting $[Ca^{2+}]_i$ may be further divided into speract-responsive and speract-nonresponsive subpopulations, the former comprising between 40–100% (median 95%, $n = 18$) of the sperm with low levels of resting $[Ca^{2+}]_i$. We noted that the proportion of speract nonresponsive cells in each batch of sperm increased as the sea urchin season progressed, though we do not know whether speract responsiveness correlated with the ability of sperm to successfully fertilize eggs.

Fig. 1 B illustrates the same sperm field as in Fig. 1 A, 4 s after exposure to 125 nM speract. Of the cells in Fig. 1 A that have low resting $[Ca^{2+}]_i$, ~95% respond to speract addition with an increase in $[Ca^{2+}]_i$. Fig. 1 C shows the Fluo-4 fluorescence increase, as measured across the whole field, in response to addition of 100 nM speract. The peak calcium increase occurs ~5 s after speract addition, and persists for upwards of 40 s. This pattern is consistent with previously published observations (Cook et al., 1994; Nishigaki et al., 2001) and indicates that the speract response of adherent sperm is similar to that seen in populations of freely swimming cells. Calcium increases in individual sperm heads were quantified using Fura-2–loaded sperm. Resting levels of $[Ca^{2+}]_i$ were 364 ± 36 nM, increasing to $1,176 \pm 112$ nM on addition of 100 nM speract ($\pm$ SEM, $n = 21$). These values are consistent with the range of values reported by previous studies (Schackmann and Chock, 1986; Cook and Babcock, 1993b; González-Martínez et al., 2001).

Imaging of single cells reveals spontaneous calcium fluctuations in resting sperm

Around 3% of sperm in the observed field in each experiment undergo spontaneous fluctuations at any given moment, and in such sperm between 1 and 5 fluctuations were recorded over a 10-s period (median = 2, $n = 33$). As noted above, 95% of sperm with low levels of resting $[Ca^{2+}]_i$ respond to speract; their response takes the form of fluctuations in the tail, with a sustained response in the head. Fig. 2 shows the kinetic characteristics of the spontaneous (A) and the speract-induced (B) $[Ca^{2+}]_i$ fluctuations. Spontaneous fluctuations have a fast rise time ($t_{1/2} = 100 \pm 20$ ms) and a relatively slow decay rate ($t_{1/2} = 900 \pm 125$ ms), and the magnitude and kinetics of these fluctuations are different from those induced by speract (compare Fig. 2 A with Fig. 2 B). Table I is a comparison of the $t_{1/2}$ of the increase and decay of individual speract-induced and spontaneous fluctuations, and a comparison of their magnitudes. All three criteria are significantly different (P < 0.001; unpaired two-tailed t test), suggesting that the mechanisms involved in the two types of $[Ca^{2+}]_i$ fluctuation are distinct (though certain ionic transporters could be shared).

The proportion of sperm undergoing spontaneous fluctuations is independent of illuminating light intensity (Table II), indicating that $[Ca^{2+}]_i$ fluctuations are not an artifact of pho-

todamage. The spontaneous increases appear to initiate first in the flagella, and then spread into the head, a pattern that has been observed at every measured spontaneous fluctuation. The spatial variations in the kinetic characteristics of the spontaneous and speract-induced $[Ca^{2+}]_i$ fluctuations are similar, and are addressed in a later section. The present paper will not deal further with the spontaneous $[Ca^{2+}]_i$ fluctuations.

Speract-induced calcium increases have superimposed tonic and phasic components

Single-cell analysis (Fig. 2 B) reveals that the speract response consists of at least two superimposed patterns of calcium increase. A sustained tonic increase occurs both in the flagella and the head cytoplasmic region. In addition, speract induces phasic $[Ca^{2+}]_i$ fluctuations superimposed on the tonic response both in the flagella and the head. The speract-induced fluctuations are smaller (Table I) and more frequent (between 10 and 20 in the first 10-s post-speract addition; Fig. 4) than the spontaneous fluctuations (1–5 over a 10-s period; $n = 34$). The $[Ca^{2+}]_i$ fluctuations in the head region were less pronounced relative to the tonic response than those in the flagella, suggesting that the head may integrate the flagellar changes. There are clear indications that the flagellar responses are correlated with the head responses, and precede them (see following section).

We have not observed any obvious correlation between sperm undergoing spontaneous fluctuations and those that respond to speract; sperm that have displayed spontaneous fluctuations can respond to speract, and cells that have not shown spontaneous fluctuations before speract addition may subsequently respond.

Analysis of calcium fluctuations in different areas of sperm indicates that the initial calcium increase propagates from flagella to head

Fig. 3 illustrates how the speract-induced $[Ca^{2+}]_i$ elevation appears to initiate in the flagella and spread from there to the head. The $t_{1/2}$ of the initial $[Ca^{2+}]_i$ elevation increases progressively with distance from the flagella (Fig. 3 A), and there is an ~1-s interval between the attainment of peak $[Ca^{2+}]_i$ in the flagellum and the tip of the head (Fig. 3 B; $n = 5$). Subsequent fluctuations show similar kinetic characteristics, as do spontaneous calcium fluctuations (unpublished data). These findings, together with those in Fig. 2, suggest that the $[Ca^{2+}]_i$ increase in the head results from the summation of $[Ca^{2+}]_i$ and/or cyclic nucleotide changes that occur in the flagella.

Both the amplitude of the tonic increase and frequency of fluctuations are dose-dependent

Both the tonic increase in $[Ca^{2+}]_i$ and the fluctuations depend on the speract concentration (Fig. 4). The speract dose dependency of the tonic calcium increases was determined by measuring $[Ca^{2+}]_i$ changes in the head (because they represent 85–95% of the total sperm signal; Fig. 4 A), whereas the frequency of the phasic fluctuations was determined from measurements on flagella (Fig. 4 B). Neither response could be detected at concentrations lower than 10 pM. The tonic response progressively increased up to 100 nM, and
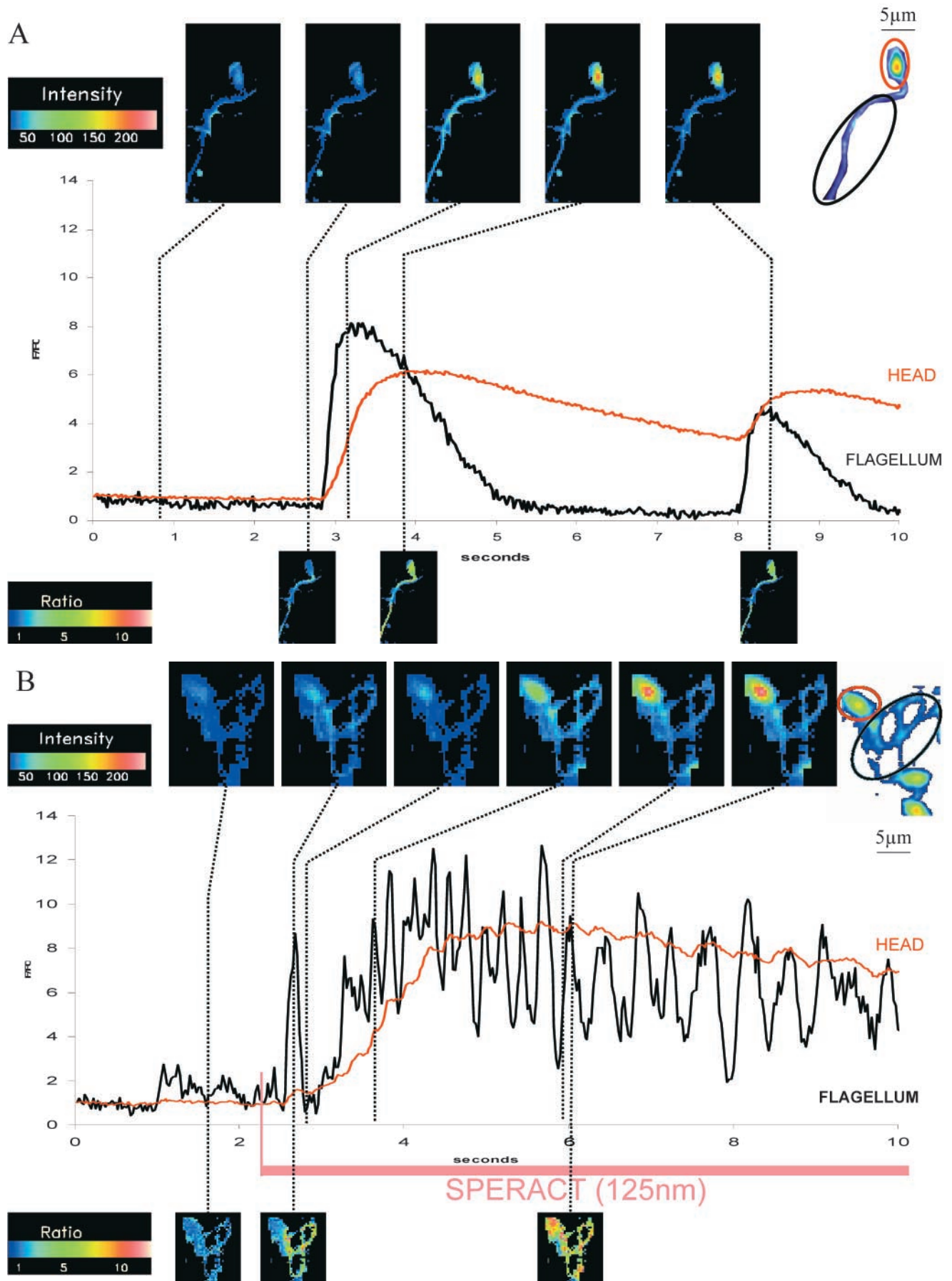
Figure 2. **Ratio increases in [Ca²⁺]ᵢ from head and flagellum regions (measured in discrete regions of interest as indicated).** Images acquired at 40 frames per second with 25-ms individual frame exposure time. (A) Typical spontaneous fluctuations in [Ca²⁺]ᵢ observed in resting sperm.

Table I. **A comparison of the kinetic characteristics of speract-induced and spontaneous fluctuations in [Ca²⁺]ᵢ**

	Speract	Control
$t_{1/2}$ increase	40 ± 5 ms	100 ± 20 ms
$t_{1/2}$ decrease	75 ± 10 ms	900 ± 125 ms
Magnitude	2.25 ± 0.01	6.8 ± 1.1

The time to reach half-height of the increase to peak, the decrease to baseline, and the overall magnitude of the fold increase in intracellular [Ca²⁺]ᵢ were measured in individual flagella. Data presented from cells treated with 100 nM speract ($n = 34$) and untreated controls ($n = 21$), where n represents a single speract-induced or spontaneous fluctuation.

Table II. **Effect of intensity of illuminating light on the proportion of sperm across fields that undergo spontaneous fluctuations**

	ND2 + 4	ND4	ND2	Direct
Number of sperm	48	51	71	56
Total number	448	469	511	511
Proportion (%)	10.71	10.87	13.89	10.96

Cells were illuminated directly, and the proportion of cells undergoing spontaneous fluctuations in a 12.5-s recording period was measured. Subsequently, neutral density (ND) filters of increasing strength (ND2, ND4, and ND2 + 4) were introduced into light path and recording was repeated as before.

the dose dependence of the tonic increase is similar to that reported in population studies, indicating the cells display a normal response to speract (Babcock et al., 1992; Schackmann and Chock, 1986). As mentioned earlier, the phasic [Ca²⁺]ᵢ fluctuations reach a maximum average number of 20 in the first 10-s post-speract addition at ∼1 nM and above.

Both tonic and phasic fluctuations are dependent on extracellular calcium

The spontaneous and speract-induced [Ca²⁺]ᵢ increases and fluctuations are completely dependent on extracellular Ca²⁺ ([Ca²⁺]ₑ). Fig. 5 shows how as [Ca²⁺]ₑ decreases, the amplitude of both the tonic response and of the fluctuations in [Ca²⁺]ᵢ induced by 1 nM speract become smaller. At 500 μM [Ca²⁺]ₑ, both the tonic and phasic responses are lost. The effect of reduction of [Ca²⁺]ₑ on the tonic response agrees with previous studies performed on sperm populations (Schackmann and Chock, 1986; Cook et al., 1994), and our results clearly indicate that Ca²⁺ influx is a major contributor to both the tonic and phasic responses.

Increasing extracellular K⁺ abolishes both tonic and phasic fluctuations, whereas removing extracellular K⁺ abolishes only the phasic component of speract-induced calcium fluctuations

Cells that undergo membrane potential (Eₘ) and [Ca²⁺]ᵢ oscillations are known to possess an appropriate battery of voltage-dependent ion channels (Gauss et al., 1998). There is evidence suggesting that sea urchin sperm posses a set of such channels: blockers of voltage-dependent cation channels (VDCCs) like Ni²⁺ and dihydropyridines, and of K⁺ channels, like TEA⁺, inhibit the acrosome reaction (AR), indicating that these channels are present in sperm. (Darszon et al., 2001). We investigated whether maneuvers that alter sperm Eₘ influence the speract-induced fluctuations in [Ca²⁺]ᵢ. The external concentration of K⁺ ([K⁺]ₑ) was varied to modify the resting and speract-induced Eₘ of sea urchin sperm (Babcock et al., 1992; González-Martínez et al., 1992). Fig. 6 shows how the magnitude of the tonic change in [Ca²⁺]ᵢ (A) and the [Ca²⁺]ᵢ fluctuations (B) induced by 500 pM speract are affected by [K⁺]ₑ. When K⁺ is removed from seawater, the speract-induced fluctuations disappear, though the tonic re-

sponse is enhanced in magnitude ($n = 35$). High [K⁺]ₑ is known to eliminate all speract responses, but the increase in cGMP (Schackmann and Chock, 1986; Harumi et al., 1992), elevating [K⁺]ₑ to 20 mM as anticipated, inhibits both tonic and phasic speract responses ($n = 68$). These findings emphasize the importance of the sperm Eₘ in the generation of the [Ca²⁺]ᵢ fluctuations as part of the speract response.

Nickel inhibits the phasic component of calcium increase

To initiate the study of the ion transport systems involved in the [Ca²⁺]ᵢ fluctuations, we tested blockers of VDCC and inhibitors of anion channels. Fig. 7 depicts the effect of 300 μM Ni²⁺, a blocker of VDCC that is more potent for T-type Ca²⁺ channels and also blocks a second poorly characterized Ca²⁺ channel involved in the sea urchin sperm AR (González-Martínez et al., 2001). Ni²⁺ at this concentration only mildly affects the tonic response, but significantly inhibits the speract-induced fluctuations in [Ca²⁺]ᵢ ($n = 28$). 300 μM Cd²⁺, which is a better blocker of L-type VDCC, was ineffective (unpublished data). Together, these data indicate that a channel with similar properties as T-type Ca²⁺ channel may be involved in generating the speract-induced [Ca²⁺]ᵢ fluctuations. Consistent with this idea, nimodipine, a Ca²⁺-channel blocker that at 10 μM can block T-type VDCC in mouse spermatogenic cells (Arnoult et al., 1997), also affected the speract-induced fluctuations (unpublished data). However, these findings do not rule out that other Ca²⁺-permeable channels (e.g., the second, Ni²⁺-sensitive channel involved in the AR; González-Martínez et al., 2001) may participate in the speract-induced [Ca²⁺]ᵢ fluctuations.

Niflumic acid increases the amplitude and periodicity of phasic fluctuations

It has been reported that sperm possess anion channels and that they may contribute to the resting Eₘ and influence the AR (Morales et al., 1993). Fig. 8 shows that niflumic acid (NA), an antagonist of anion and nonselective cation channels profoundly affects the speract-induced [Ca²⁺]ᵢ fluctuations. At a concentration of 100 μM, it significantly increases the magnitude of [Ca²⁺]ᵢ fluctuations (6.2 ± 0.3-fold increase in flagella [Ca²⁺]ᵢ; $n = 5$, $P < 0.001$; unpaired two-

Images above graphs are intensity images; images below graphs are ratio images against the frame immediately before the spontaneous increase occurred. (B) Typical response of an individual sperm to addition of speract to a final concentration of 125 nM. Images above graphs are intensity images; images below are ratio images against the frame immediately before speract addition. Note the markedly higher intensity of the head compared with the tail and that the fold increases in head and tail are comparable.
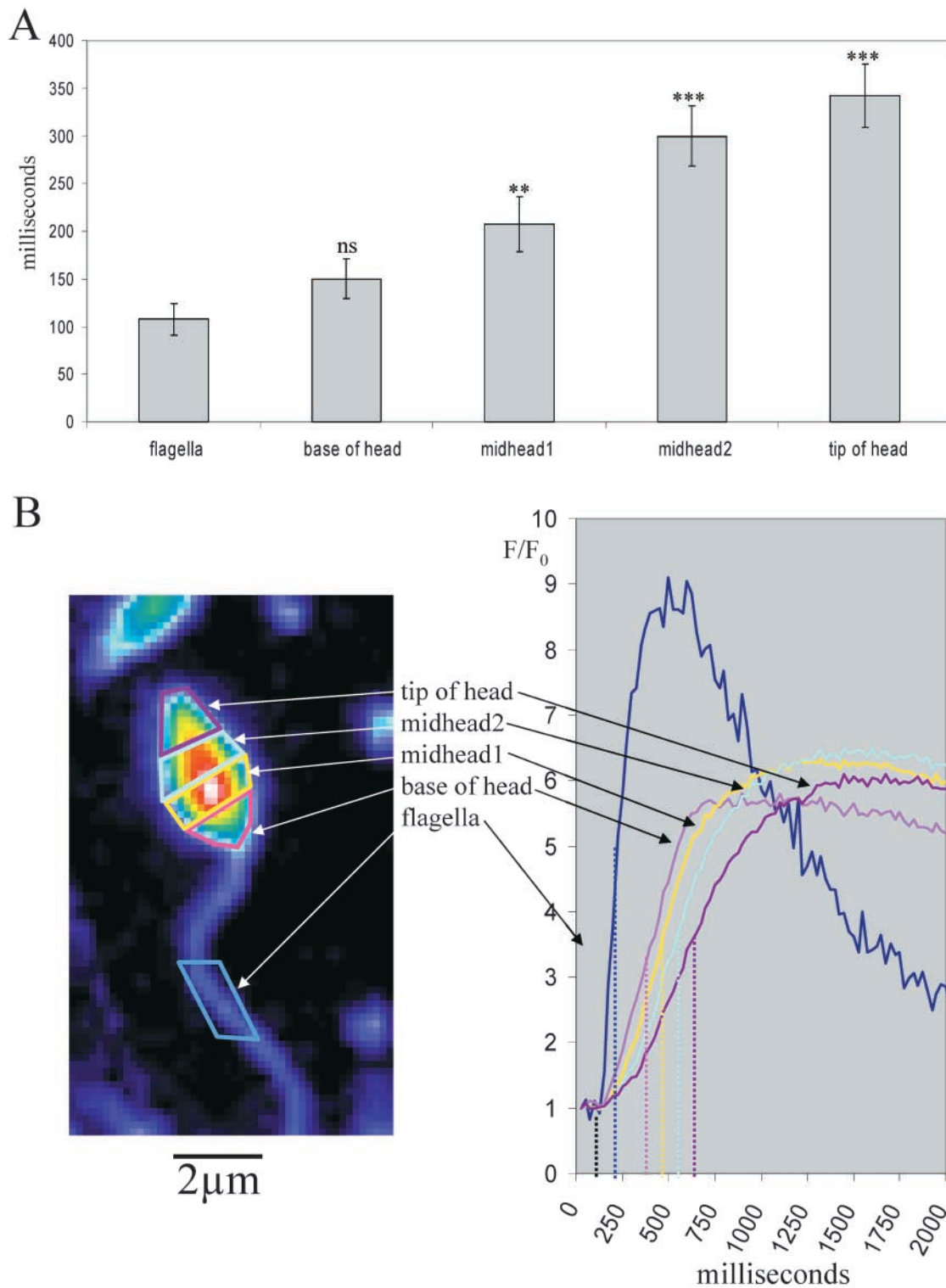
Figure 3.   **Subregional analysis of $[Ca^{2+}]_i$ increases in individual sperm.** (A) After addition of 100 nM speract, the time taken for the initial calcium increase to reach half height (relative to the first point of increase in the flagellum) was recorded for subregions of the sperm head and flagellum (B); $n = 5$, error bars indicate ± SEM. One-tailed t test (comparison to flagellum). ***, P < 0.001; **, P < 0.01; ns, P > 0.05.

tailed t test, in comparison with Table II) and reduces their frequency (2.4 ± 0.3 fluctuations per 10-s post-1 nM speract addition; $n = 5$, P < 0.001; unpaired two-tailed t test, in comparison with Fig. 4 B). These results suggest that anion channel(s) are important elements of a pacemaker-type mechanism that may underlie the speract-induced fluctuations.

IBMX abolishes the phasic component of speract-induced calcium fluctuations, alters kinetics of tonic response, and reduces level of $[Ca^{2+}]_i$ in flagella

Speract elevates the levels of cGMP and cAMP. These second messengers then modulate sperm ion permeability (reviewed in Darszon et al., 2001). To explore how the levels of these cyclic
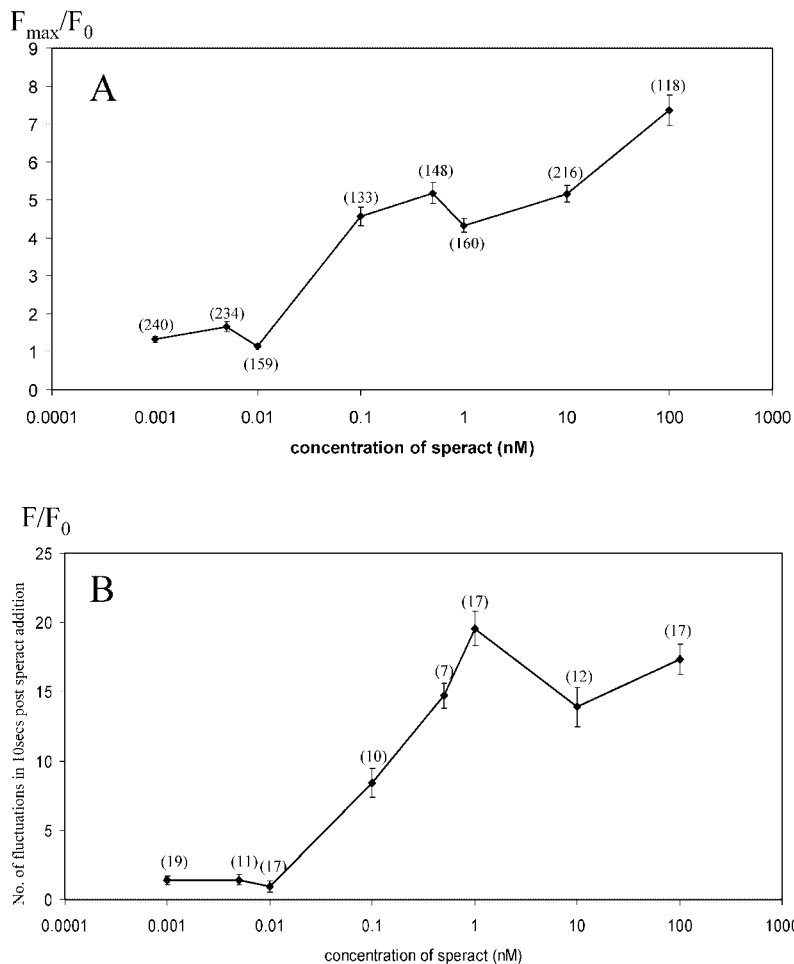
F_{max}/F_0

A

F/F_0

B

Figure 4. **The magnitude of the tonic calcium increase and the frequency of the phasic calcium fluctuations are dependent on the concentration of speract.** (A) For each sperm head, the ratio increase in $[Ca^{2+}]_i$ was determined from the maximum fluorescence intensity post-speract addition (F_{max}) and the initial fluorescence intensity value (F_0). F_{max}/F_0 is presented as the average of all sperm heads analyzed (total number of sperm heads at each speract concentration shown in brackets). Error bars indicate $\pm$ SEM. At concentrations of speract above and including 100 pM, only those sperm heads that showed a response to speract were analyzed. At concentrations of speract below and including 10 pM, and in control analyses, sperm heads were chosen at random. (B) Changes in $[Ca^{2+}]_i$ were determined for individual flagella by ratioing their fluorescence (F) against their initial fluorescence (F_0). The number of fluctuations occurring after speract addition was determined by including all excursions whose increase from trough to peak was >20% of the trough value. Data are presented as the average number of fluctuations occurring in 10 s post-speract addition per flagellum. Number of flagella analyzed indicated in brackets. Error bars represent $\pm$ SEM.

nucleotides affect the speract-induced $[Ca^{2+}]_i$ fluctuations, we used 3-isobutyl-1-methylxanthine (IBMX), an inhibitor of cyclic nucleotide phosphodiesterases (Cook and Babcock, 1993a,b). As illustrated in Fig. 9 A, 100 μM IBMX abolishes the speract-induced $[Ca^{2+}]_i$ fluctuations, but not the sustained $[Ca^{2+}]_i$ increase in the head. However, the kinetic characteristics of the tonic $[Ca^{2+}]_i$ increase are altered significantly: $t_{1/2}$ of tonic elevation in $[Ca^{2+}]_i$ is 6.5 $\pm$ 0.25 s in IBMX-treated sperm versus 0.98 $\pm$ 0.25 s in non-IBMX–treated sperm ($n =$ 17, P < 0.001; unpaired two-tailed t test). In the flagella (Fig. 9 B), the speract-induced phasic fluctuations are abolished, and the small tonic increase in calcium, although sustained, does not gradually increase over time as in the head ($n = 8$).

Discussion

Speract-induced calcium increases in sperm populations result from heterogeneous responses at the level of single sperm

The aggregate calcium signal that we record in a population of adherent sperm in response to speract corresponds very closely in time course, magnitude, and dose-response properties to the population calcium response previously measured in sperm suspensions (Babcock et al., 1992; Schackman and Chock, 1986). However, analysis of the calcium response at the single-cell level shows a degree of heterogeneity unsuspected from measurements in sperm populations. One sperm

subpopulation consists of sperm with unvarying, high levels of calcium. These may represent sperm that loose their capacity to regulate $[Ca^{2+}]_i$, perhaps through interaction with the polylysine-treated glass coverslip; however, it is of course unknown whether this subpopulation is also present in the sperm suspensions studied previously; with current imaging methods, it is not possible to track calcium dye signals in free-swimming sperm. The second major subpopulation consists of sperm with low resting levels of calcium. The majority of these cells respond to speract, though we noted that the proportion of cells responding declined as the breeding season progressed. It was also noteworthy that the level of responsiveness of the responders was relatively uniform, allowing this population with low resting calcium concentrations to be readily classified into responders and nonresponders. Again, this information has been unavailable in previous studies. The most striking heterogeneity we observed was in the spatiotemporal pattern of the calcium response to speract in single sperm. We also observed spontaneous calcium increases with equivalent spatiotemporal heterogeneity.

Calcium increases occur first in the sperm tail, then in the head

Close inspection of both spontaneous and speract-induced calcium increases showed that an interval of ~1 s elapsed between the calcium increase in the tail and that at the tip of the head; the increase in the flagella was synchronous at the 25-ms

Figure 5. **Speract-induced increases in $[Ca^{2+}]_i$ are dependent on $[Ca^{2+}]_e$ in a dose-dependent manner.** (A) For each sperm head, the ratio increase in $[Ca^{2+}]_i$ was determined from the maximum fluorescence intensity after addition of speract to a final concentration of 1 nM (F_{max}) and the initial fluorescence intensity value (F_0). F_{max}/F_0 is presented as the average of all sperm heads analyzed (total number of sperm heads at each $[Ca^{2+}]_e$ shown in brackets). Error bars represent ± SEM. (B) Typical responses in individual sperm heads at different $[Ca^{2+}]_e$. F/F_0 shown over time after addition of speract to a final concentration of 1 nM (indicated by arrow) and data represented as a five-point rolling average. Images acquired at 10 frames per second with 100-ms individual frame exposure time. One-tailed t test (comparison to prior $[Ca^{2+}]_e$) **, P < 0.01; *, P < 0.05.
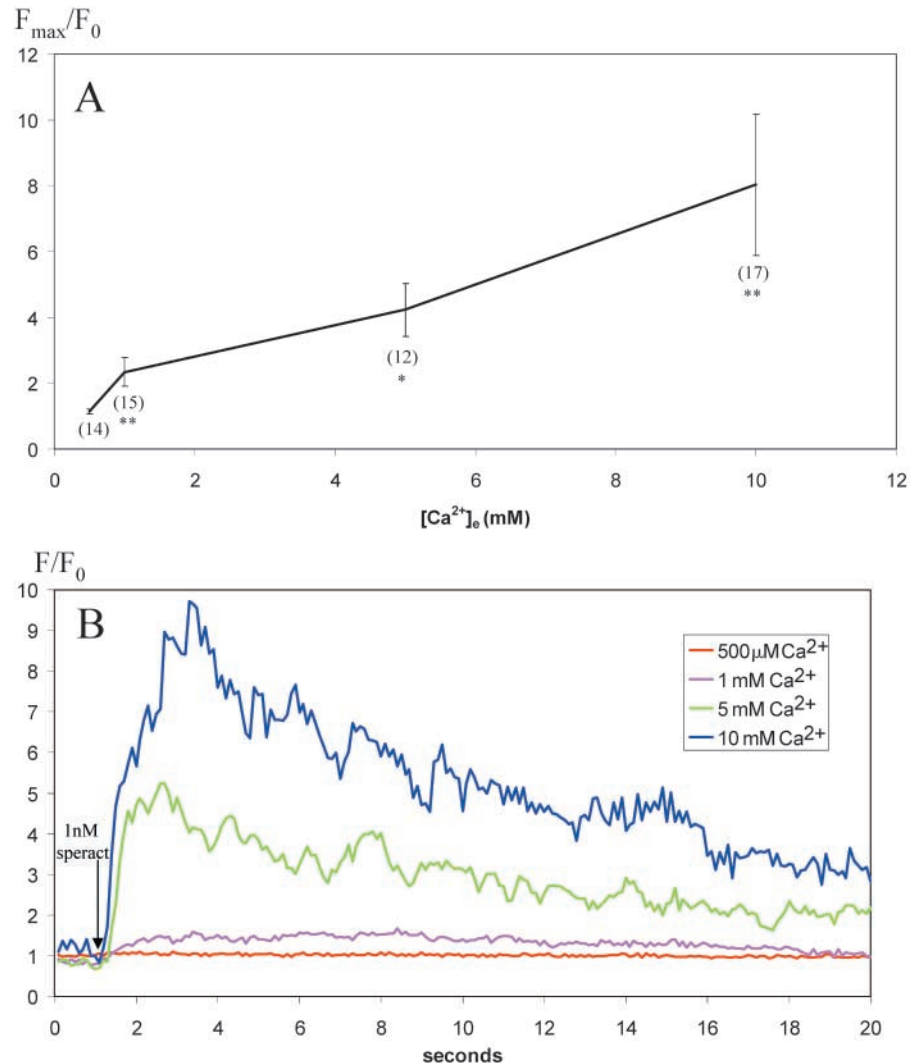
time resolution of our experiments. Analysis of the calcium increase in response to speract in head and tail revealed that the response comprised two elements: a tonic response on which was superimposed phasic fluctuations. In the tail, the phasic component predominated, whereas in the head, the tonic component was much more marked, with phasic fluctuations superimposed on a monotonically increasing component that rose to a plateau. As speract concentrations were increased, the phasic component showed an increased frequency (measured in the tail), whereas the tonic component showed an increased magnitude (measured in the head), both over the range of speract concentrations known to modulate the calcium response from experiments in sperm suspensions.

It occurred to us that a simple explanation that might account for these results was that a signal originated periodically in the tail in response to speract and diffused to the head, where it was summed or integrated. This simple hypothesis is supported by quantitative modeling (Fig. 10), though by itself this by no means constitutes proof.

Another major difference between head and tail calcium signals was their relative contribution to the whole-sperm calcium signal. The majority of the calcium reporter dye signal (∼85%) is localized to the head. Thus, irrespective of whether a single wavelength or ratio calcium dye is used, the calcium concentration in the head contributes disproportionately to the whole-sperm calcium signal. Therefore, calcium measurements in sperm suspensions largely report calcium in the head.

Ionic basis of the tonic and phasic responses

Both tonic and phasic components of the calcium response to speract were reduced proportionately by reduction of extracellular calcium, disappearing at ∼0.5 mM $[Ca^{2+}]_e$, consistent with previous work in suspensions (Schackmann and Chock, 1986). This result demonstrates that the phasic responses in the tail and the tonic response in the head both require calcium influx. High potassium sea water abolished the speract response completely, as has been reported previously (Lee and Garbers, 1986; Schackmann and Chock, 1986; Babcock et al., 1992); under these conditions, the only intracellular response to speract is an increase in cGMP (Harumi et al., 1992).

The calcium channel blocker Ni^{2+} abolishes the phasic response to speract, but not the tonic response. The anion channel blocker niflumic acid markedly enhances the phasic responses in both head and tail and reduces their frequency.

These observations suggest a mechanism in which the phasic tail responses are sensitive to membrane potential and ion fluxes. A simple hypothesis consistent with these finding
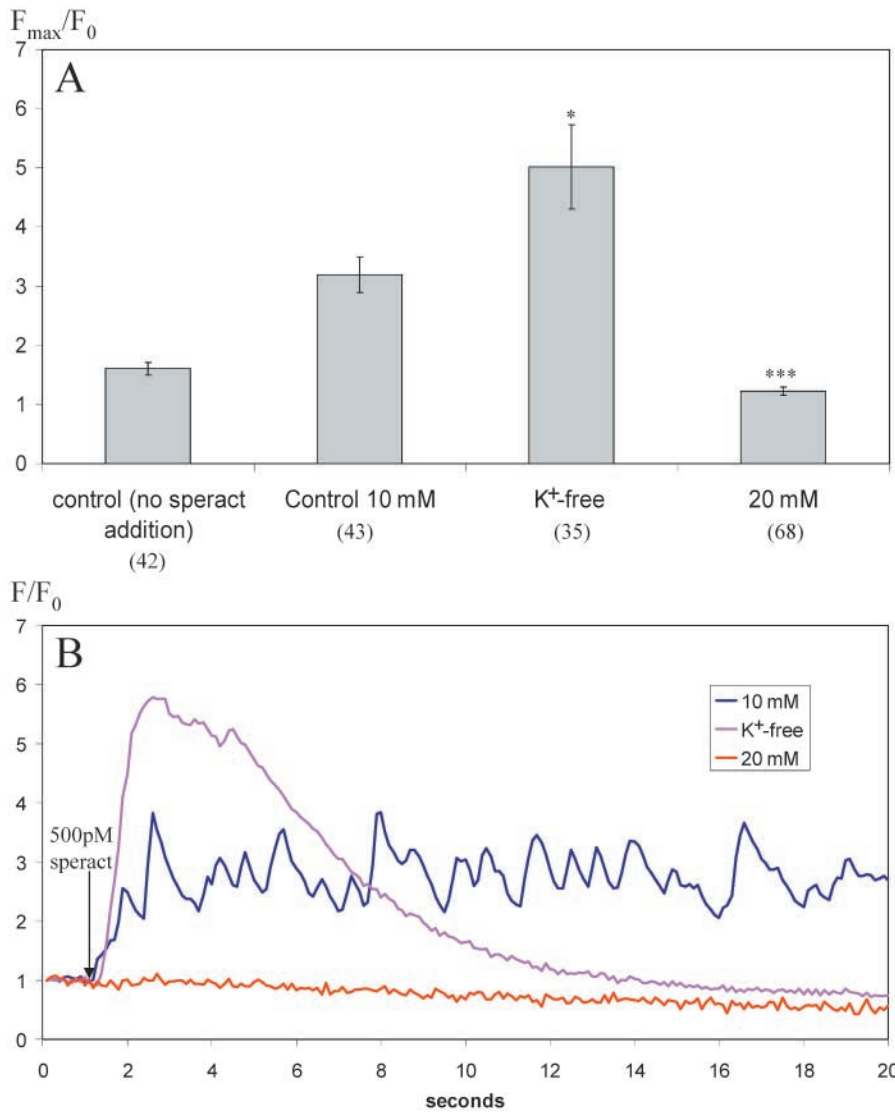
Figure 6. **The degree and characteristics of speract-induced increases in $[Ca^{2+}]_i$ are altered by both increasing and decreasing $[K^+]_e$.** (A) For each sperm head, the ratio increase in $[Ca^{2+}]_i$ was determined from the maximum fluorescence intensity after addition of speract to a final concentration of 500 pM (F_{max}) and the initial fluorescence intensity value (F_0). F_{max}/F_0 is presented as the average of all sperm heads analyzed (total number of sperm heads at each $[K^+]_e$ shown in brackets). Error bars represent ± SEM. (B) Typical responses in individual sperm heads at different $[K^+]_e$. F/F_0 shown over time after addition of speract to a final concentration of 500 pM (indicated by arrow). Images acquired at 10 frames per second with 100-ms individual frame exposure time. One-tailed *t* test (comparison to 10 mM data) ***, P < 0.001; *, P < 0.05.

is that the fluctuating calcium responses in the tail are driven or terminated by membrane potential changes, and that a component of this mechanism is driven by calcium influx through a Ni^{2+}-sensitive voltage-gated calcium channel in the tail, but essentially absent in the head because the tonic response in the head is unaffected by Ni^{2+}. The enhance-
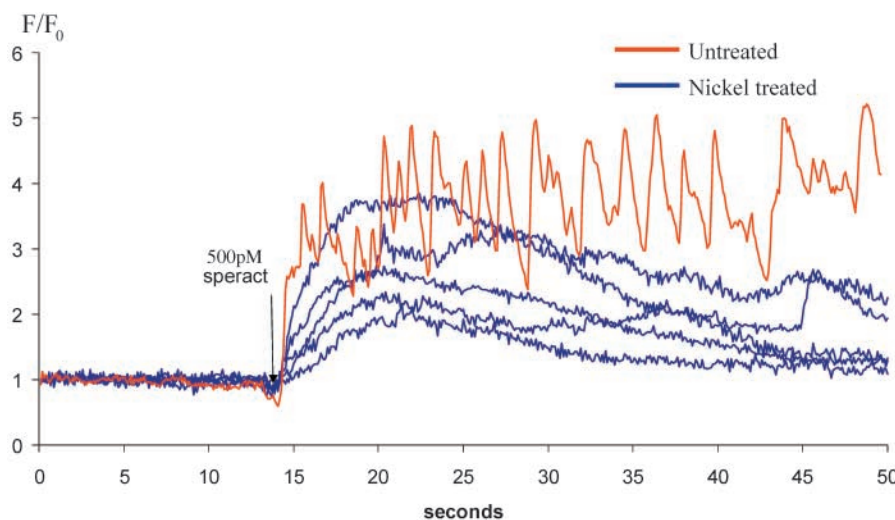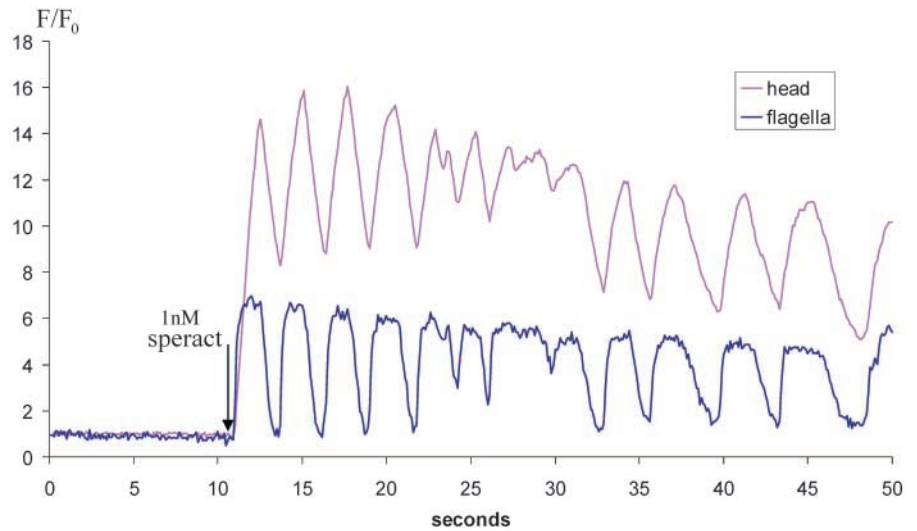

Figure 7. **Representative examples of the effect of Ni^{2+} treatment on speract-induced $[Ca^{2+}]_i$ increases in individual sperm heads.** Blue traces from sperm treated with 300 μM Ni^{2+} before addition of 500 pM speract (indicated by arrow); red trace from untreated sperm. Changes in $[Ca^{2+}]_i$ were determined for individual heads by ratioing their fluorescence (F) against their initial fluorescence (F_0). Images acquired at 10 frames per second with 100-ms individual frame exposure time.

Figure 8. **Representative example of the effect of niflumic acid treatment on speract-induced [Ca^{2+}]$_i$ increases in individual sperm.** Sperm treated with 100 μM niflumic acid before addition of 1 nM speract (indicated by arrow). Changes in [Ca^{2+}]$_i$ were determined for heads and flagella by ratioing their fluorescence (F) against their initial fluorescence (F$_0$).


ment of the fluctuations after treatment with niflumic acid suggests that the membrane potential changes can be modulated by inhibition of anion channels.

Role of cyclic nucleotides

It is generally accepted that the first response to speract in sperm is the generation of cGMP, through activation by the

Figure 9. **Representative examples of the effect of IBMX treatment on speract-induced [Ca^{2+}]$_i$ increases in individual sperm.** (A) Effect of IBMX treatment on Ca^{2+} increase in sperm heads. Images acquired at 10 frames per second with 100-ms individual frame exposure time. (B) Effect of IBMX treatment on [Ca^{2+}]$_i$ increase in sperm flagella. Images acquired at 40 frames per second with 25-ms individual frame exposure time. In both A and B, blue traces from sperm treated with 100 μM IBMX before addition of 500 pM speract (indicated by arrow); red trace from non-IBMX–treated sperm. Changes in [Ca^{2+}]$_i$ were determined for heads and flagella by pseudo-ratioing their fluorescence (F) against their initial fluorescence (F$_0$).
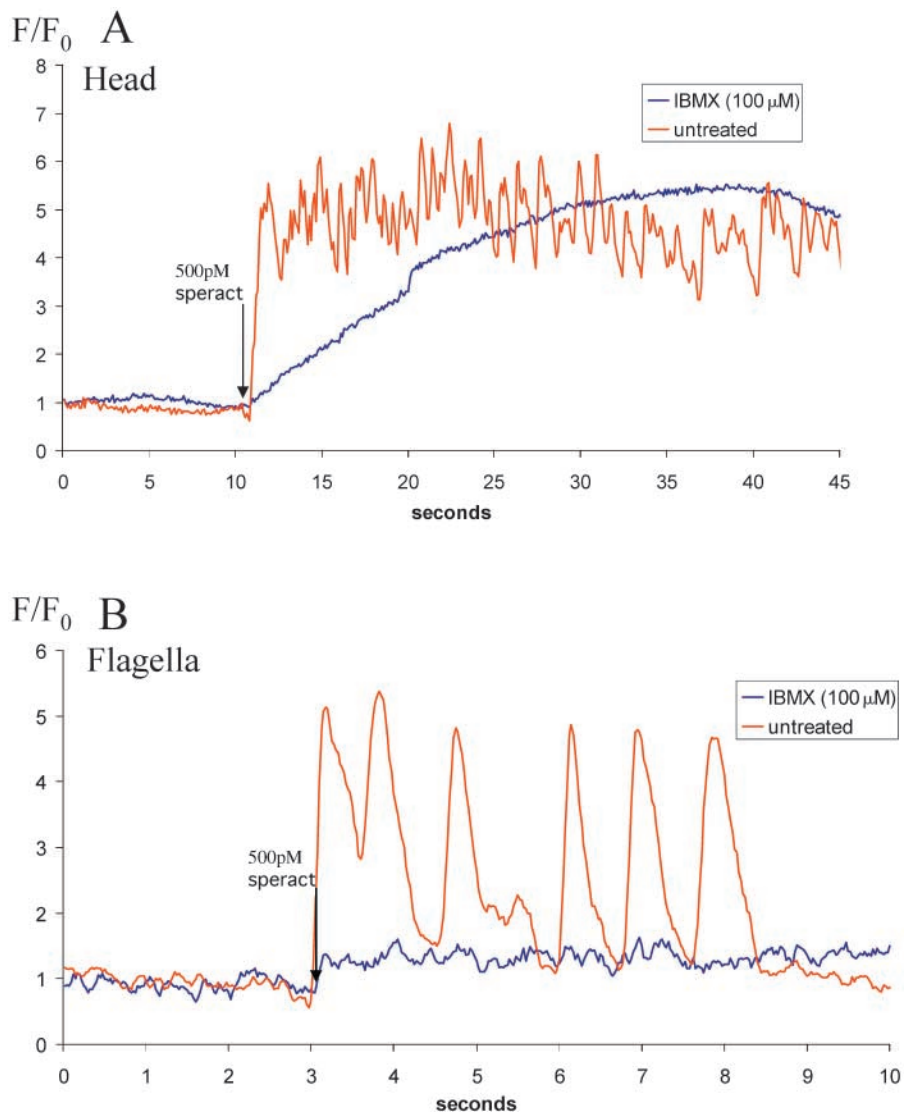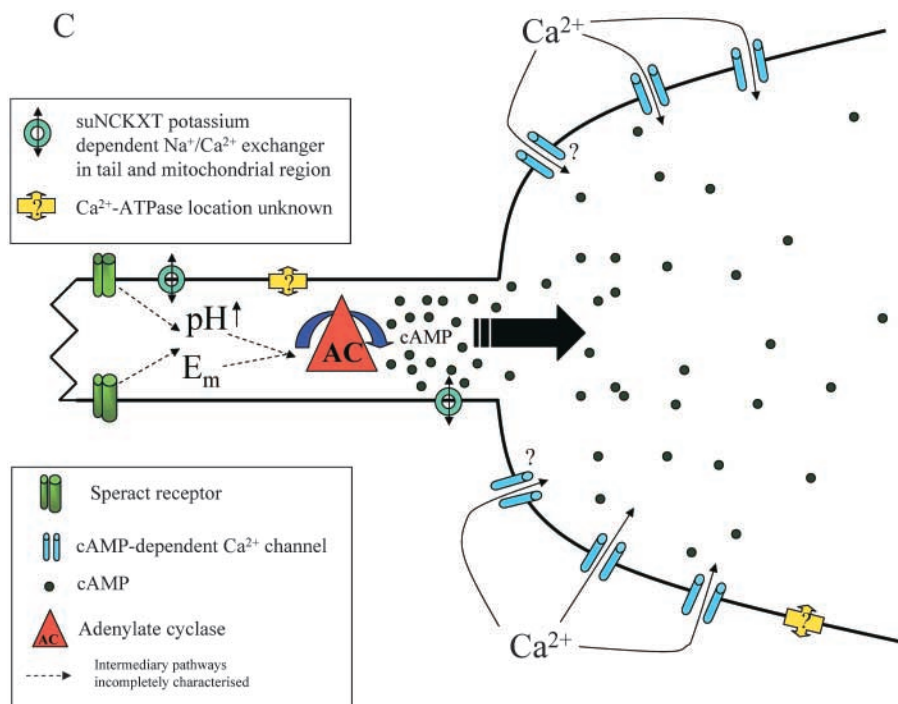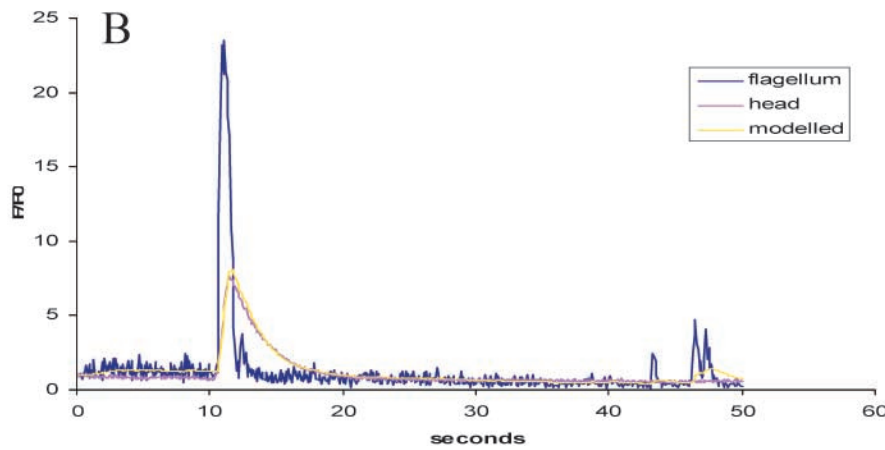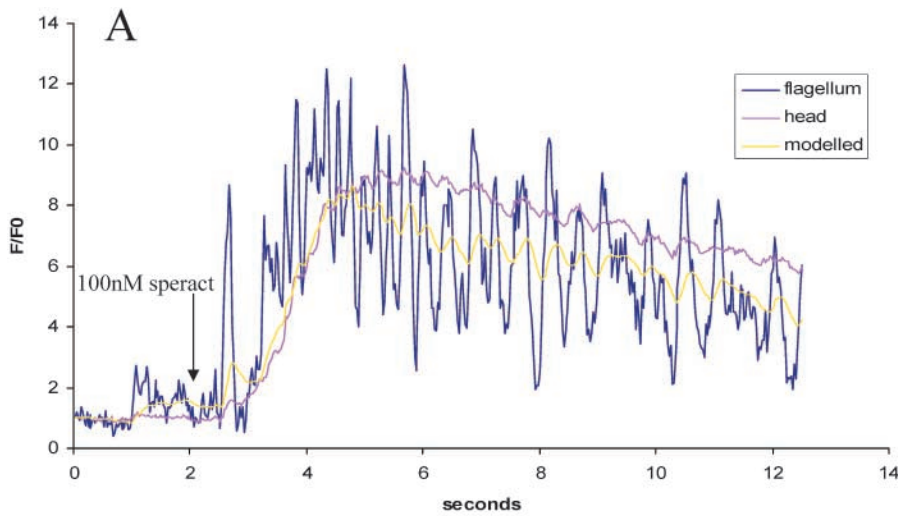
Figure 10. **Quantitative modeling of calcium changes in the head of individual sperm undergoing speract-induced and spontaneous increases in [Ca^{2+}]$_i$.** For details of the model, see Materials and methods. (A) Typical increase in [Ca^{2+}]$_i$ of sperm treated with 100 nM speract (indicated by arrow) with increases in both head and tail. The increase in the head can be modeled by diffusion from the tail through a bottleneck with an apparent rate constant of 2 s^{-1}. (B) Typical increase in [Ca^{2+}]$_i$ of sperm undergoing spontaneous fluctuation, with the increase in the head modeled using the same rate constant. Modeling suggests that extrusion or destruction of the diffusing signal is not significant on these timescales. (C) Schematic diagram showing proposed model of speract-induced Ca^{2+} entry into the heads of sea urchin sperm. Activation of the speract receptor localized to the flagellum results in up-regulation of the activity of adenylate cyclase, also predominantly localized to the flagellum, via increases in pH, [Ca^{2+}]$_i$ and/or changes in E$_m$. cAMP then diffuses into the head, opening the cAMP-dependent Ca^{2+} channels localized there. Calcium efflux pathways are also shown.

speract receptor of a guanylate cyclase localized to the tail. Changes in pH_i and E_m then activate an adenylate cyclase (Beltran et al., 1996), mainly found in the flagella (Toowicharanont and Shapiro, 1988), that has been postulated to open cAMP-activated Ca^{2+} channels (Cook and Babcock, 1993b). We treated sperm with IBMX, a phosphodiesterase inhibitor that in sea urchin sperm prevents the hydrolysis of cGMP and cAMP (Cook and Babcock, 1993a). We found that the phasic response was abolished completely in the tail and replaced by a small, sustained Ca^{2+} increase, whereas in the head Ca^{2+} rose around six times more slowly than in controls, but to levels comparable or greater than the control maximum. These results suggest that the cAMP-gated Ca^{2+} influx mechanism is more prominent in the head than in the tail. It is interesting to note that in *A. punctulata* sperm suspensions, the kinetics of the Ca^{2+} response are much more rapid after uncaging caged cGMP than after uncaging caged cAMP (Kaupp et al., 2003).

A model for the spatial regulation of the Ca^{2+} response in single sperm

Our analysis of Ca^{2+} signaling patterns in response to speract in single sperm suggest four main hypotheses. The first is that E_m changes in the tail are linked to the predominantly tail-localized Ca^{2+} fluctuations. The second is that the voltage-dependent calcium channels that drive the fluctuations are located in the tail, as the tail fluctuations can be blocked by inhibitors of certain voltage-activated Ca^{2+} channels (Ni^{2+}, and to a lesser degree nimodipine), whereas the tonic increases in the head, though dependent on Ca^{2+} influx, are unaffected. The third is that the activation of the calcium pathway invariably spreads from tail to head, suggesting that the early components of the response that drive the fluctuations are restricted to the tail. The fourth is that preventing the hydrolysis of cGMP and cAMP lead to loss of tail fluctuations and a much slower tonic rise in calcium in the head.

These hypotheses suggest a model in which the cGMP-induced membrane potential changes generate tail calcium fluctuations and drive the production of cAMP, which then diffuses from the tail into the head. The model is supported by the observation that in high K^+ sea water, which allows only the initial cGMP increase but prevents changes in both membrane potential and cAMP (see model in Cook and Babcock, 1993b), speract addition fails to generate a calcium increase in the tail, let alone the head.

The importance of the fluctuations in driving the head calcium response is underlined by the consequences of treatment with IBMX. Though levels of both cGMP and cAMP are enhanced (Cook and Babcock, 1993b; Beltrán et al., 1996), the calcium response (and so presumably the cAMP response) is very substantially slowed.

It is interesting to consider the mechanism by which the head might integrate the speract response. One obvious possibility is that calcium increases in the tail diffuse slowly into the head region. This seems to us unlikely on two grounds. The first is that the calcium concentrations in head and tail seem comparable, not differing by the 10-fold or more that would be necessary to fit a calcium diffusion model. The second is that we have detected no gradient of calcium concentration in the tail. Because the tail is long and thin and has a much smaller volume than the head, it is difficult to see how sub-

stantial diffusion of calcium from tail to head could occur without the appearance of a gradient in the tail. A more attractive explanation is that the diffusing vector is cAMP, generated as pulses in the tail in synchrony with the calcium fluctuations. cAMP then gates cAMP-dependent calcium channels preferentially located in the head. Why does the head integrate the tail-derived signals? Our model suggests that it is because there is a diffusion bottleneck at the point that the tail joins the head. Other explanations are possible: for example, the calcium extrusion mechanisms may have a lower capacity in the head than in the tail, or phosphodiesterase activity may be lower in the head than the tail. Because calcium decreases faster during oscillations in the tail than in the head, we favor the former as more reasonable; the surface/volume ratio of the head is far higher than the tail, so that the condition would apply even at constant extrusion activity per membrane surface area. In fact, it is possible that intrinsic extrusion rates are higher in the tail than the head, for although the sperm Ca^{2+}-ATPase (Garcia-Soto et al., 1988) localization is unknown, it has been shown that a potassium-dependent Na^+/Ca^{2+} exchanger (suNCKXT) is localized to the tail and mitochondrial region and is absent in the head (Su and Vacquier, 2002). Moreover, modulating Na^+/Ca^{2+} exchanger activity alters the kinetics of the speract response in cell populations (Rodriguez and Darszon, 2003). The latter explanation is also possible, as our simple model shows that there little loss of the diffusing substance in the head itself; decreases in the head are modeled by diffusion back into the tail through the bottleneck, rather than by degradation in the head. A model for the spatial localization of the elements of the speract response mechanism is shown as Fig. 10 C.

Speract and motility

It remains to be shown that speract acts in sperm-egg chemotaxis like its analogue resact (Ward et al., 1985; Kaupp et al., 2003). Nonetheless, there is evidence that speract can modulate sperm motility (Cook et al., 1994). Modulation of sperm swimming behavior is thought to occur at the level of the axoneme, and indeed, calcium is known to modulate the beat characteristics of sea urchin sperm (Brokaw, 1987; Cosson, 1996). The generally unspoken assumption in experiments in which calcium is measured in sperm populations is that speract-induced calcium increases are occurring in the tail, in contrast to those involved in the acrosome reaction that take place in the head (Cook et al., 1994; Darszon et al., 2001). It is now clear that the calcium signal measured in experiments with sperm populations is predominantly from the head. It seems very likely that the phasic tail responses that we have uncovered will play a vital role in modulating sperm swimming behavior in response to speract.

Materials and methods

Gamete handling
Sperm were obtained "dry" from *S. purpuratus* (Marinus, Inc.) by intercolecomic injection of 0.5 M KCl and stored on ice.

Materials
Artificial seawater (ASW) contained (mM): 430 NaCl, 10 KCl, 10 $CaCl_2$, 23 $MgCl_2$, 25 $MgSO_4$, 2 $NaHCO_3$, and 1 EDTA (pH 8.0, 950–1000 mosM). Low Ca^{2+} ASW (pH 7.0) was as ASW but at pH 7.0 and with 1 mM $CaCl_2$, and Ca^{2+}-free ASW was ASW with no added $CaCl_2$. K^+-free ASW was pre-

pared as ASW but omitting KCl, and high K$^+$ ASW was prepared as ASW but with 20 mM KCl. Fura-2 AM, Fluo-4 AM, and pluronic F-127 were from Molecular Probes, Inc. IBMX, ionomycin, NiCl$_2$, niflumic acid, and poly-D-lysine were from Sigma-Aldrich. Speract was synthesized in Dr. Possani's laboratory as described previously (Nishigaki et al., 2001).

Loading of fluorescent indicators (AM esters) into sperm

Dry sperm were suspended in 10 volumes of low Ca^{2+} ASW (pH 7.0) containing 0.5% wt/vol pluronic F-127 and 20 μM of either Fura-2 AM or Fluo-4 AM and incubated for 2–3 h at 16°C. Loaded sperm were then diluted with 10 volumes low Ca^{2+} ASW (pH 7.0), centrifuged for 10 min at 1,000 g and 4°C, and resuspended in the original volume of low Ca^{2+} ASW (pH 7.0). Sperm were stored in the dark and on ice until use.

Single-cell imaging

Imaging chambers were prepared by coating coverslips with 50 μg/ml poly-D-lysine, shaking off excess, and allowing to air-dry. Coated coverslips were then attached to Perspex rings with high vacuum silicon grease to form watertight chambers. Labeled sperm were diluted 1:20 to 1:40 in ASW, immediately placed into the chambers, and left for 1–3 min, after which unattached sperm were removed by washing with ASW. The chambers were then filled with 1 ml of the appropriate medium (if not ASW, 3 × 1-ml washes were performed with appropriate medium). Chambers were then mounted on a microscope (Diaphot 300; Nikon) with a 40× fluor objective, and fluorescence changes were recorded on a camera (Coolsnap-FX; Photometrics) used in continuous (stream) acquisition mode.

Image processing

Images were processed offline using MetaMorph® (Universal Imaging). Rolling background subtraction was performed using a region of interest placed as close as possible to the sperm of interest. Any incompletely adhered sperm that moved during the course of any experiment were discounted. Fluorescence measurements in individual sperm were made by manually drawing a region of interest around the head or a section of flagella for each sperm. Measurements were taken from head or flagella regions as indicated in the figure legends. All measurements of speract-induced or spontaneous fluctuations were taken from flagella. A fluctuation was defined as an excursion whose increase from trough to peak was >20% of the trough value.

Determination of [Ca^{2+}]$_i$

The majority of data presented were obtained using Fluo-4–loaded sperm. These are presented as pseudoratios as indicated on the individual figures. [Ca^{2+}]$_i$ was determined from Fura-2 measurements according to the following formula: [Ca^{2+}]$_i$ = K$_d$(R − R$_{min}$)/(R$_{max}$ − R)(F$_b$380/F$_f$380). The ratiometric 340/380 value R$_{max}$ and F$_b$380 (fluorescence at 380 excitation) were obtained when calcium-saturated by the addition of 2 μM ionomycin in ASW. R$_{min}$ and F$_f$380 were obtained after addition of 2 μM ionomycin in Ca^{2+}-free ASW supplemented with 10 mM EGTA. K$_d$ = 774 nM (Poenie et al., 1985).

Modeling of [Ca^{2+}]$_i$ increases in sperm heads

It was assumed that calcium changes in the head were driven by diffusion of a substance down a concentration gradient from tail to head and that a second process removed the substance from the head by extrusion or metabolism. An approximate model of these processes is provided by the differential equation: dy/dt = k$_1$ · (u − y) – k$_2$ · y, where y is the concentration of a substance in the head and u is the concentration of the same substance in the tail. k$_1$ and k$_2$ are rate constants. This differential equation was solved using a Runge-Kutta approach.

References

Arnoult, C., J.R. Lemos, and H.M. Florman. 1997. Voltage-dependent modulation of T-type calcium channels by protein tyrosine phosphorylation. *EMBO J.* 16:1593–1599.

Babcock, D.F., M.M. Bosma, D.E. Battaglia, and A. Darszon. 1992. Early persistent activation of sperm K$^+$ channels by the egg peptide speract. *Proc. Natl. Acad. Sci. USA.* 89:6001–6005.

Beltrán, C., O. Zapata, and A. Darszon. 1996. Membrane potential regulates sea urchin sperm adenylylcyclase. *Biochemistry.* 35:7591–7598.

Brokaw, C.J. 1979. Calcium-induced asymmetrical beating of triton-demembranated sea urchin sperm flagella. *J. Cell Biol.* 82:401–411.

Brokaw, C.J. 1987. Regulation of sperm flagellar motility by calcium and cAMP-dependent phosphorylation. *J. Cell Biochem.* 35:175–184.

Cardullo, R.A., S.B. Herrick, M.J. Peterson, and L.J. Dangott. 1994. Speract receptors are localized on sea urchin sperm flagella using a fluorescent peptide analog. *Dev. Biol.* 162:600–607.

Cook, S.P., and D.F. Babcock. 1993a. Selective modulation by cGMP of the K$^+$ channel activated by speract. *J. Biol.Chem.* 268:22402–22407.

Cook, S.P., and D.F. Babcock. 1993b. Activation of Ca^{2+} permeability by cAMP is coordinated through the pHi increase induced by speract. *J. Biol. Chem.* 268:22408–22413.

Cook, S.P., C.J. Brokaw, C.H. Muller, and D.F. Babcock. 1994. Sperm chemotaxis: egg peptides control cytosolic calcium to regulate flagellar responses. *Dev. Biol.* 165:10–19.

Cosson, J. 1996. A moving image of flagella: news and views on the mechanisms involved in axonemal beating. *Cell Biol. Int.* 20:83–94.

Darszon, A., C. Beltran, R. Felix, T. Nishigaki, and C.L. Trevino. 2001. Ion transport in sperm signaling. *Dev. Biol.* 240:1–14.

Garcia-Soto, J., M. Mourelle, I. Vargas, L. de la Torre, E. Ramirez, A.M. Lopez-Colome, and A. Darszon. 1988. Sea urchin sperm head plasma membranes: characteristics and egg jelly induced Ca^{2+} and Na$^+$ uptake. *Biochim. Biophys. Acta.* 944:1–12.

Gauss, R., R. Seifert, and U.B. Kaupp. 1998. Molecular identification of a hyperpolarization-activated channel in sea urchin sperm. *Nature.* 393:583–587.

González-Martinez, M.T., A. Guerrero, E. Morales, L. de De La Torre, and A. Darszon. 1992. A depolarization can trigger Ca^{2+} uptake and the acrosome reaction when preceded by a hyperpolarization in *L. pictus* sea urchin sperm. *Dev. Biol.* 150:193–202.

González-Martinez, M.T., B.E. Galindo, L. de De La Torre, O. Zapata, E. Rodriguez, H.M. Florman, and A. Darszon. 2001. A sustained increase in intracellular Ca^{2+} is required for the acrosome reaction in sea urchin sperm. *Dev. Biol.* 236:220–229.

Harumi, T., K. Hoshino, and N. Suzuki. 1992. Effects of sperm-activating peptide I on *Hemicentrotus pulcherrimus* spermatozoa in high potassium sea water. *Dev. Growth Differ.* 34:163–172.

Kaupp, U.B., J. Solzin, E. Hildebrand, J.E. Brown, A. Helbig, V. Hagen, M. Beyermann, F. Pampaloni, and I. Weyand. 2003. The signal flow and motor response controling chemotaxis of sea urchin sperm. *Nat. Cell Biol.* 5:109–117.

Lee, H.C., and D.L. Garbers. 1986. Modulation of the voltage-sensitive Na$^+$/H$^+$ exchange in sea urchin spermatozoa through membrane potential changes induced by the egg peptide speract. *J. Biol. Chem.* 261:16026–16032.

Morales, E., L. de la Torre, G.W. Moy, V.D. Vacquier, and A. Darszon. 1993. Anion channels in the sea urchin sperm plasma membrane. *Mol. Reprod. Dev.* 36:174–182.

Nishigaki, T., F.Z. Zamudio, L.D. Possani, and A. Darszon. 2001. Time-resolved sperm responses to an egg peptide measured by stopped-flow fluorometry. *Biochem. Biophys. Res. Commun.* 284:531–535.

Poenie, M., J. Alderton, R.Y. Tsien, and R.A. Steinhardt. 1985. Changes of free calcium levels with stages of the cell division cycle. *Nature.* 315:147–149.

Rodriguez, E., and A. Darszon. 2003. Intracellular sodium changes during the speract response and the acrosome reaction in sea urchin sperm. *J. Physiol.* 546:89–100.

Schackmann, R.W., and P.B. Chock. 1986. Alteration of intracellular [Ca^{2+}] in sea urchin sperm by the egg peptide speract. Evidence that increased intracellular Ca^{2+} is coupled to Na$^+$ entry and increased intracellular pH. *J. Biol. Chem.* 261:8719–8728.

Su, Y.H., and V.D. Vacquier. 2002. A flagellar K($^+$)-dependent Na($^+$)/Ca(2$^+$) exchanger keeps Ca(2$^+$) low in sea urchin spermatozoa. *Proc. Natl. Acad. Sci. USA.* 99:6743–6748.

Suarez, S.S., S.M. Varosi, and X. Dai. 1993. Intracellular calcium increases with hyperactivation in intact, moving hamster sperm and oscillates with the flagellar beat cycle. *Proc. Natl. Acad. Sci. USA.* 90:4660–4664.

Toowicharanont, P., and B.M. Shapiro. 1988. Regional differentiation of the sea urchin sperm plasma membrane. *J. Biol. Chem.* 263:6877–6883.

Ward, G.E., C.J. Brokaw, D.L. Garbers, and V.D. Vacquier. 1985. Chemotaxis of *Arbacia punctulata* spermatozoa to resact, a peptide from the egg jelly layer. *J. Cell Biol.* 101:2324–2329.